

## ANALYSIS OF FLOOD AND WATER IMPACT ON THE NEW AIRPORT PROJECT IN BEIHAI CITY

<sup>1,2</sup>Tang, C.\*, <sup>1</sup>Ngien, S.K.

<sup>1</sup>Faculty of Civil Engineering Technology, Universiti Malaysia Pahang al-Sultan Abdullah,  
Malaysia

<sup>2</sup>College of Civil and Architectural Engineering, NanNing University, China.

\* Corresponding Author: [396805005@qq.com](mailto:396805005@qq.com) TEL: +86-15296486180

Received: 15 December 2024; Accepted: 7 March 2025; Published: Date: 30 June 2025

doi: 10.35934/segi.v10i1.119

---

### Highlights:

- One-Dimensional and Two-Dimensional water flow modelling using MIKE software.
- Simulation of levee-break flooding superimposed with regional waterlogging.
- Beihai Airport project as a reference for flood risk and control of similar projects.

---

**Abstract:** With the frequent occurrence of extreme rainfall events worldwide, the problem of floods and water disasters has become increasingly prominent. During the construction of engineering projects, it is necessary to fully analyze the situation of regional floods and water disasters, provide a basis for the design of flood control and drainage plans for the main project, and ensure the safety of project operation. Taking Beihai Airport Project in southern China as the study area, this paper analyzes the flood situation in the project area under the condition of 100-year return period design flood and the condition of 100-year return period design flood plus 100-year return period design rainstorm. Modelling results showed that the submerged depth within the site range from 0 to 1.32m, Distributed in the southwest, central, and eastern parts of the airport area. The tributary of Hougang River passes through the airport construction area, when encountering a 100-year flood, The flood will overflow the riverbank and enter the airport construction area. Flood prevention measures need to be considered during airport construction. This study provides a basis for the design of airport flood control and waterlogging drainage scheme, and also provides a reference for the analysis of waterlogging impact of similar projects.

Keywords: Numerical; Simulation; River Breach; Waterlogging; Flood Routing

---

## 1. Introduction

### 1.1. Research Background

Beihai City is located in the southern part of Guangxi, China, on the northeast coast of the Beibu Gulf. The city is positioned as an international coastal tourism destination and a regional

international tourism distribution service center, mainly for leisure and vacation. It is an important gateway to the 21st century "Maritime Silk Road". Beihai City is the only coastal city in western China to be included in the first batch of 14 cities to further open up to the outside world. It is also the only city in southern China to have a deep-water port, all-weather airport, railway, and expressway at the same time. According to the forecast released by government departments, by 2030, the total population of Beihai City will reach 3.2 million, and the number of tourists will exceed 50 million. The development potential of civil aviation is huge. According to the regional development plan, Beihai City plans to build a new airport in the Northwest to meet the development requirements of the regional tourism market.

The proposed new airport is located in Hepu County, Beihai City, with the runway direction running Southwest-Northeast. The proposed location is mainly surrounded by rivers such as the Hougang River, Hongchao River, and Xiatun River. The Hougang River and Xiatun River are both located near bays. Due to the shape, terrain, and characteristics of both river basins, the drainage capacity of the river channel themselves are relatively low. In the case of continuous heavy rainfall, the flood discharge of the river channels are not timely, and it is easy to overflow the river embankment, forming a dam break. Heavy downpour will cause waterlogging disasters in the region. The floods that occur often covers the entire river basin. With the frequent occurrence of extreme rainfall events worldwide, the problem of flood disasters has become increasingly prominent, causing significant loss of life and economic damage (Hosseinzadehtalaei et al., 2021).

## 1.2. Current Research Status

Numerical simulation has been widely studied and applied in dam-break flood research globally due to its advantages of strong flexibility, low cost, short cycle, and independence from experimental site limitations. Scholars have developed various models for dam-break flood analysis, such as the DWOPER, DAMBRK, FLDWAV, HEC-RAS, and MIKE21 models (Li Yang, 2021). These models have facilitated extensive research on flood evolution mechanisms (Seyedashraf et al., 2012; Ghaeini-Hessaroeiyeh et al., 2022). For example, Xueyao & Cheng (2019) utilized numerical models to investigate the impact of different breach evolution processes on flood propagation, revealing correlations between flood characteristics and breach forms, locations, and quantities (Xueyao & Cheng ,2019). Wanlin & Zhen (2022) employed the MIKE21 model to construct a flood evolution model, analyzing inundation risks in estuarine areas (Wanlin & Zhen , 2022). Similarly, Hasibuan et al. (2022) applied HEC-RAS to assess flood inundation depth and area risks in specific regions (Hasibuan et al. , 2022).

In urban waterlogging analysis, models such as MIKE, SWMM, and InfoWorks ICM are widely adopted and have demonstrated effectiveness in flood prevention (Wang et al., 2015). For instance, Min et al. (2022) used ICM software to simulate extreme rainfall scenarios in Wuhan, identifying key inundation zones and analyzing drainage processes (Min et al. , 2022). Chen & Zhao (2022) explored rainwater flow patterns through T-SAS model experiments, providing insights for mitigating waterlogging disasters (Chen & Zhao, 2022). Wei et al. (2022) developed a coupled 1D-2D urban flood model using InfoWorks ICM, highlighting the influence of rainfall duration and intensity on flood depth and persistence (Wei et al., 2022). Yang et al. (2022) further applied this model to predict future urban waterlogging risks, offering guidance for infrastructure planning (Yang et al., 2022).

In summary, theoretical research on flood mechanisms has established a relatively comprehensive framework. In urban planning and disaster mitigation, the application of hydrodynamic simulation software (e.g., MIKE21 FM) has proven effective in evaluating flood vulnerability and designing countermeasures. This study adopts MIKE21 FM to simulate waterlogging and flood evolution in the proposed airport area, aiming to provide scientific guidance for airport construction and enhance infrastructure resilience, while offering references for similar projects.

## **2. Numerical Simulation Analysis of Floods**

### **2.1. Assessment of Flood Breach Location**

The focus of this study is on the flood and waterlogging inundation issues of the proposed airport site. Therefore, the proposed airport site is taken as the center, covering the surrounding major river areas as the spatial limits of the research. The study area and its surrounding watershed water system are shown in **Figure 1**.

According to the evaluation of the surrounding water system in the study area, there are two rivers with external flood possibility in the study area, namely the Hougang River and Xiatus River, and a water diversion channel named Hongchao West Main Canal. There is a large reservoir located at its upper reaches that has an established flow regulation regime and ample storage capacity. In the event of a major flood, it can ensure safe flow discharge and the downstream will be almost unaffected. Therefore, the impact of the flood collapse from Hongchao West Main Canal can be ignored.

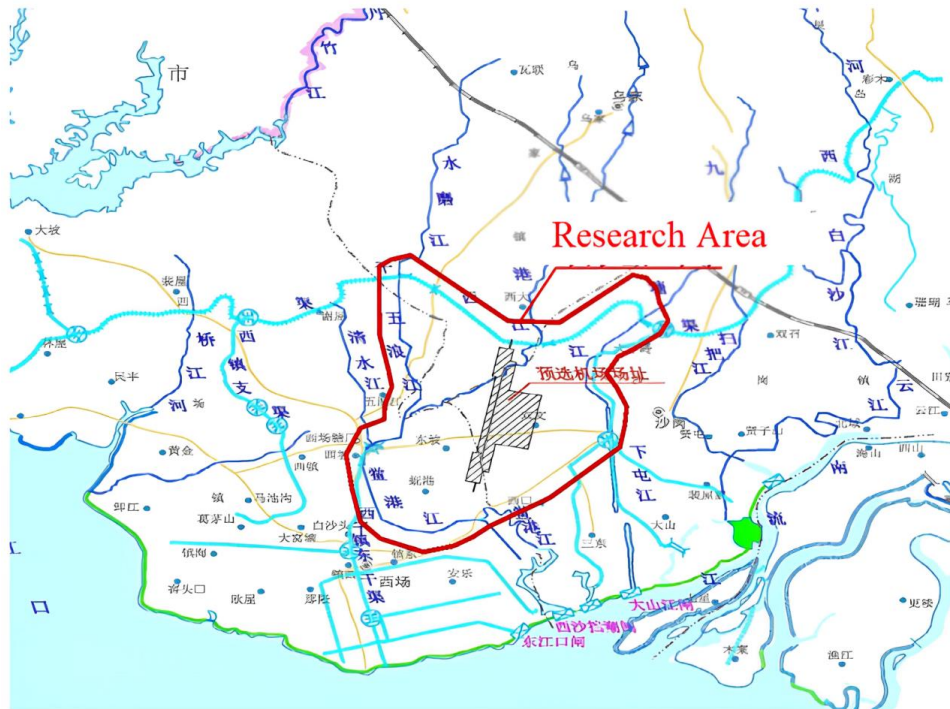


**Figure 1.** Study area and surrounding river basin water system

Hougang River and Xiatun River are currently in their natural state without any embankment construction. When encountering floods, the bends of the rivers are subject to the dual effects of flood crest and scouring which makes it easy to cause riverbank collapse. Based on the worst-case scenario that will affect the airport, a breach was established in the main stream of Hougang River, the left tributary of Hougang River, and the area with the weakest flood erosion of Xiatun River. The locations of the river breach is detailed in **Figure 2**.

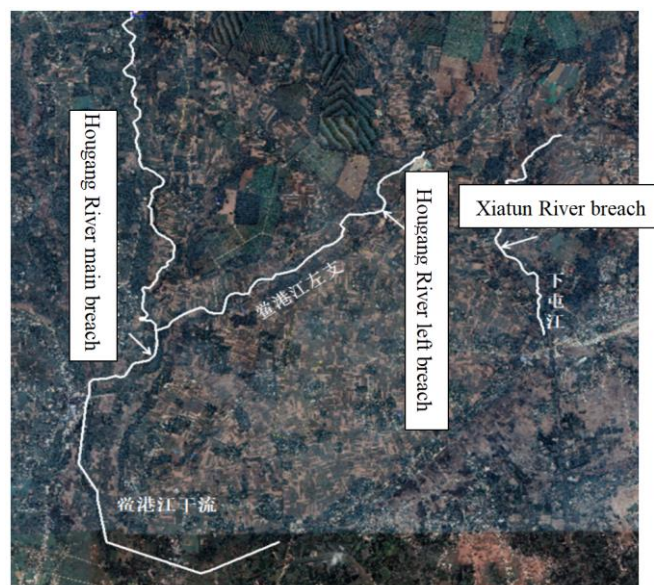


**Figure 2.** Locations of the river breach

### 2.2. Governing Equations

The analysis of the flood process at the breach site is carried out using the MIKE11 hydrodynamic model. The basic principle is to assume that the water flow is an incompressible and homogeneous fluid, and to simulate and analyze it using the Saint Venant equation system. The specific form of the equation system is as follows:

Continuous equation (1):

$$\frac{\partial Q}{\partial x} + \frac{\partial A}{\partial t} = q \tag{1}$$

Momentum equation (2):

$$\frac{\partial Q}{\partial t} + \frac{\partial}{\partial x} \left( \frac{\alpha Q^2}{A} \right) + gA \frac{\partial Z}{\partial x} + g \frac{Q|Q|}{C^2 AR} = 0 \tag{2}$$

In the formula:  $Q$  is the flow rate,  $m^3/s$ ;  $A$  is the cross-sectional area of the discharge,  $m^2$ ;  $q$  is the lateral inflow flow rate,  $m^3/s$ ;  $\alpha$  is the momentum correction coefficient;  $Z$  is the water level,  $m$ ;  $g$  is the acceleration due to gravity,  $m/s^2$ ;  $C$  is the Chezy Coefficient;  $R$  is the hydraulic radius,  $m$ .

The model adopts a six point Abbott-Ionescu finite difference scheme to discretize the Saint Venant equation system. This discrete format alternately calculates water level or flow rate in sequence at points along the flow path, referred to as point  $h$  and point  $Q$  respectively, as shown in **Figure 3**.

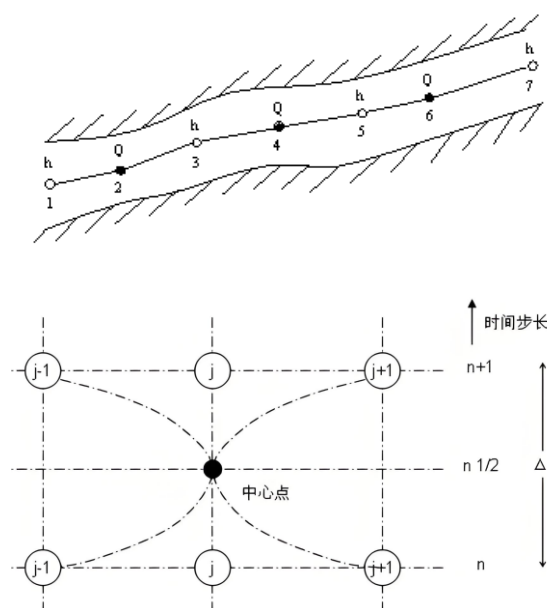


**Figure 3.** Abbott format water level point, flow point alternating layout diagram

The evolution analysis after flood breach is simulated using the MIKE21 FM model. The principle of MIKE21 FM hydrodynamic module is based on the two-dimensional incompressible fluid Reynolds averaged stress equation and follows the Boussinesq assumption and hydrostatic pressure assumption. The control equation is as follows:

Continuous equation (3) of water flow:

$$\frac{\partial Z}{\partial t} + \frac{\partial}{\partial x}(ZU) + \frac{\partial}{\partial y}(ZV) = ZS \quad (3)$$

Equation (4-6) of water flow momentum:

$$\frac{\partial ZU}{\partial t} + \frac{\partial ZU^2}{\partial x} + \frac{\partial VU}{\partial y} = fVZ - gZ \frac{\partial \eta}{\partial x} - \frac{Z \partial p_a}{\rho_0 \partial x} - \frac{gZ^2}{2\rho_0} \frac{\partial \rho}{\partial x} + \quad (4)$$

$$\frac{\tau_{ax}}{\rho_0} - \frac{\tau_{bx}}{\rho_0} - \frac{1}{\rho_0} \left( \frac{\partial s_{xx}}{\partial x} + \frac{\partial s_{xy}}{\partial y} \right) + \frac{\partial}{\partial x}(ZT_{xx}) + \frac{\partial}{\partial y}(ZT_{xy}) + Zu_s S$$

$$\frac{\partial ZV}{\partial t} + \frac{\partial ZUV}{\partial x} + \frac{\partial V^2}{\partial y} = fUZ - gZ \frac{\partial \eta}{\partial y} - \frac{Z \partial p_a}{\rho_0 \partial y} - \frac{gZ^2}{2\rho_0} \frac{\partial \rho}{\partial y} + \quad (5)$$

$$\frac{\tau_{ay}}{\rho_0} - \frac{\tau_{by}}{\rho_0} - \frac{1}{\rho_0} \left( \frac{\partial s_{yx}}{\partial x} + \frac{\partial s_{yy}}{\partial y} \right) + \frac{\partial}{\partial x}(ZT_{xy}) + \frac{\partial}{\partial y}(ZT_{yy}) + Zv_s S$$

$$ZU = \int_{-d}^{\eta} u dz \quad ZV = \int_{-d}^{\eta} v dz \quad (6)$$

In the formula, x, y, and z are Cartesian coordinates; U, V is the flow velocity based on the average water depth; t is time;  $\tau$  is the shear stress; s is the size of point source traffic;  $\eta$  is the elevation of the riverbed; d is the depth of still water; Z is the total head,  $Z=\eta+d$ ; u and v are the velocity components in the x and y directions; g is the acceleration due to gravity;  $\rho$  is the density of water;  $s_{xx}$ ,  $s_{xy}$ ,  $s_{yx}$ , and  $s_{yy}$  are the components of radiation stress;  $T_{xx}$ ,  $T_{xy}$ , and  $T_{yy}$  are components of shear force in different directions;  $p_a$  is atmospheric pressure;  $\rho_0$  is the relative density of water;  $u_s$  and  $v_s$  are the flow velocities of the source sink water flow.

## 2.3. Model Setup

### 2.3.1. Grid Division

In consideration of the actual topographical and hydrological conditions of the project area, In creating terrain files, the boundary line xyz file is first imported into the Mesh Generator module of MIKE Zero to generate the boundary of the study area after which the equidistant

boundary lines are inserted before the downstream river outlet position of the study area is defined as the open boundary and the mesh is generated.

The model mesh division adopts irregular triangular mesh. Considering that the refinement of the mesh is proportional to the subsequent simulation calculation time, this paper has generated a total of 17098 meshes, with an average mesh area of  $0.00414 \text{ km}^2$ , a maximum mesh area of  $0.00896 \text{ km}^2$ , a minimum mesh area of  $0.00106 \text{ km}^2$ , and a total mesh area of  $70.77 \text{ km}^2$ . Based on the rule of thumb widely practiced in the industry, the size of the model grid should be controlled within  $0.05 \text{ km}^2$  when simulating two-dimensional flood routing. The grid size division of the model in this paper meets the requirements.

Due to the impact of the quality of terrain files on the stable operation of subsequent simulations, Analyze Mesh is used after the mesh division is completed to check the quality of the mesh division and fine tune the meshes with poor quality. After the grid division is completed, the elevation point xyz file is imported into the Mesh Generator module and a terrain file is generated through scatter interpolation.

The completed terrain file is shown in **Figure 4**.

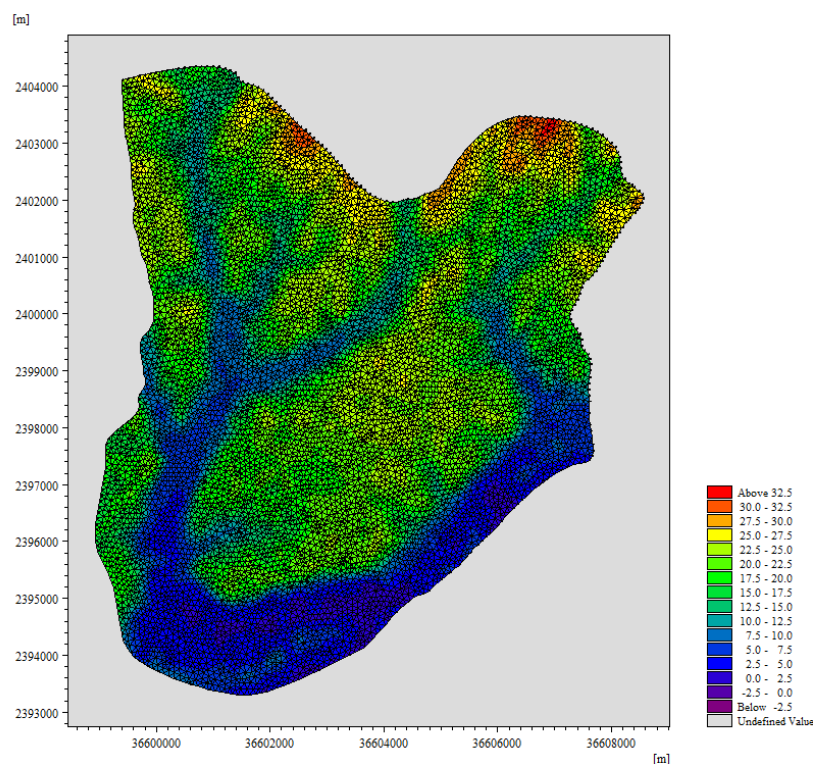


**Figure 4.** Simulated regional topographic map

### 2.3.2. Roughness Analysis

The roughness value is based on the land use division results, referring to the roughness values of various types of land as well as to Li (2006). The roughness values of various types of land in this article are shown in **Table 1**. The detailed division of land use in the research area is shown in **Figure 5**.

**Table 1.** Study area roughness n value table

Land classification	Cultivated land	Residential area	Woodland	Grass	Unused land
Value	0.06	0.1	0.1	0.05	0.03

### 2.3.3. Parameter Settings

- 1) Time step size. In two-dimensional simulation, the Courant-Friedrichs-Lewy (CFL) value is related to the grid size and time step. If the CFL value is greater than 1, the stability and accuracy of the numerical simulation cannot be guaranteed, and the time step needs to be reduced. However, if the time step is too small, it will increase the calculation time of the model. Therefore, considering the stability calculation time of the model, the time step is determined to be 60s.
- 2) Model dynamic boundary setting. Due to the presence of dynamic boundaries within the simulation area that vary with water level fluctuations, continuity of model calculations is ensured by setting the dry and wet water depths using default parameters in the two-dimensional model, with dry water depth  $h_{dry} = 0.005\text{m}$ , submerged water depth  $h_{floud} = 0.05\text{m}$ , and wet water depth  $h_{wet} = 0.1\text{m}$ . When the water depth in the calculation area is less than  $0.005\text{m}$ , the calculation area is considered "dry" and is removed from the calculation. When the water depth in the calculation area is greater than  $0.1\text{m}$ , the calculation area is considered "wet" and needs to participate in the calculation.
- 3) Coriolis Force. The Coriolis force is related to geographic information, and since the terrain file in this article sets a spatial coordinate system, it is not necessary to set the Coriolis force.
- 4) Others. The selection of other parameters such as eddy viscosity coefficient, wind field, ice cover, and radiation waves needs to be set according to the characteristics of different modules and simulation areas. Due to the small overall impact of other parameters on this study, default data are used for the aforementioned parameters.

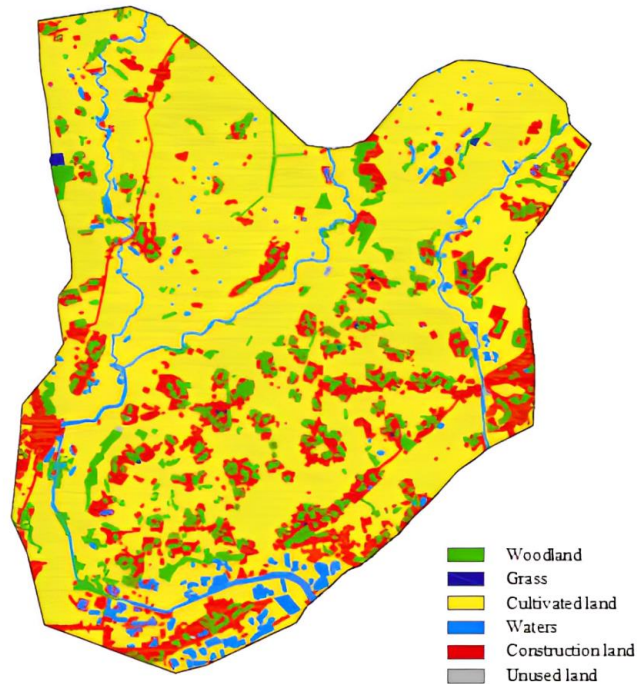


**Figure 5.** Regional land use division

## 2.4 Model Calibration

After the model construction is completed, the model is calibrated based on historical flood data before setting the breach. The calibration follows the accuracy requirements for model verification specified in the Guidelines for Flood Risk Mapping (2005) and the Technical Specifications for Flood Risk Mapping, which state that for river floods, the maximum water level error (the absolute maximum difference between the measured and calculated water levels) at internal stations and along the flood marks should be  $\leq 20$  cm.

### (1) Xiatun River

According to historical flood survey data, at the 2198m point of the Xiatun River model, the measured maximum water level of a 100-year flood event once reached 12.38 meters. In the one-dimensional simulation without a breach, when the roughness coefficient of the Xiatun River was 0.024, the water level at this location was 12.371 m; when the roughness coefficient was 0.025, the water level was 12.394 m. Due to insufficient calibration data, to reduce errors and improve calibration accuracy, further simulations were conducted for the roughness coefficient range of 0.024~0.025, ultimately determining a roughness coefficient of 0.0244.

## (2) Main Stream of Hougang River

According to historical flood survey data, at the 2198-meter mark of the main stream model of the Hougang River, the measured water level of a 100-year flood event once reached 7.87 meters. In the model, when the roughness coefficient of the main stream of the Hougang River was 0.023, the water level at 7914 m was 7.80 m; when the roughness coefficient was 0.024, the water level was 7.86 m; and when the roughness coefficient was 0.025, the water level was 7.929 m. Further simulations were conducted for the roughness coefficient range of 0.024~0.025, ultimately determining a roughness coefficient of 0.0241.

## (3) Left Branch of Hougang River

According to historical flood survey data, at the 2380-meter mark of the left branch model of the Hougang River, the measured water level of a 100-year flood event once reached 11.09 meters. In the model, when the roughness coefficient of the left branch of the Hougang River was 0.023, the water level at 2380 m was 11.055 m; when the roughness coefficient was 0.024, the water level was 11.116 m. Further simulations were conducted for the roughness coefficient range of 0.023~0.024, ultimately determining a roughness coefficient of 0.0236.

## 3. Result and Analysis

### 3.1. Results of One-Dimensional Model

Through one-dimensional model calculations, the water flow processes of the upstream breach of the Hougang River, the downstream breach of the Hougang River, and the Xiatus River breach are shown in **Table 2**. The peak and total flood volume of each breach are shown in **Table 3**.

The results of the one-dimensional model's breach flow process are added as the inflow boundary conditions of the two-dimensional model and simulated to obtain the evolution process of the breach flood in the area modelled.

### 3.2. Two-Dimensional Model Results

The maximum submerged depth of the two-dimensional model is shown in **Figure 6**. In order to illustrate the inundation situation within the proposed airport site, the vertex numbers of the site boundary are set as 1-12, and the two locations with the highest inundation depth within the site are numbered as 13 and 14, respectively. The specific numbering and location of the locations with larger inundation depth are shown in **Figure 7**, while the inundation depth and water level results of typical locations around the site are shown in **Table 4**.

**Table 2.** Water flow process of each breach

Time t (h)	Process of breach flow (m <sup>3</sup> /s)			Time t (h)	Process of breach flow (m <sup>3</sup> /s)		
	Hougang River left breach	Hougang River main breach	Xiatun River breach		Hougang River left breach	Hougang River main breach	Xiatun River breach
0	0.15	0.17	0.10	37	6.91	7.58	3.51
1	0.90	0.98	0.52	38	6.70	7.35	3.41
2	2.50	2.67	1.38	39	6.50	7.12	3.30
3	10.03	10.88	5.91	40	6.30	6.91	3.21
4	42.95	46.61	25.35	41	6.11	6.70	3.11
5	95.86	104.09	54.56	42	5.93	6.50	3.02
6	132.44	144.01	72.63	43	5.75	6.31	2.93
7	147.77	160.93	78.49	44	5.58	6.12	2.84
8	148.38	161.86	76.77	45	5.41	5.93	2.76
9	138.93	151.79	70.19	46	5.25	5.76	2.67
10	122.25	133.79	60.32	47	5.09	5.59	2.60
11	103.33	113.27	49.90	48	4.94	5.42	2.52
12	85.32	93.67	40.47	49	4.79	5.26	2.44
13	69.65	76.57	32.58	50	4.65	5.10	2.37
14	56.73	62.43	26.28	51	4.51	4.95	2.30
15	46.00	50.66	21.14	52	4.38	4.80	2.23
16	36.74	40.50	16.72	53	4.25	4.66	2.17
17	29.12	32.13	13.14	54	4.12	4.52	2.11
18	23.20	25.61	10.43	55	4.00	4.38	2.04
19	18.83	20.78	8.48	56	3.88	4.26	1.98
20	15.74	17.36	7.16	57	3.77	4.13	1.93
21	13.66	15.04	6.31	58	3.65	4.01	1.87
22	12.33	13.55	5.80	59	3.56	3.90	1.82
23	11.54	12.66	5.52	60	3.52	3.85	1.80
24	11.13	12.19	5.41	61	3.47	3.80	1.78
25	10.99	12.02	5.41	62	3.43	3.76	1.76
26	10.33	11.36	5.13	63	3.39	3.71	1.74
27	9.81	10.77	4.90	64	3.35	3.67	1.72
28	9.37	10.29	4.70	65	3.31	3.63	1.70
29	9.00	9.87	4.53	66	3.27	3.58	1.68
30	8.67	9.51	4.38	67	3.23	3.54	1.66
31	8.37	9.18	4.23	68	3.20	3.50	1.64
32	8.09	8.87	4.10	69	3.16	3.46	1.62
33	7.83	8.59	3.97	70	3.12	3.42	1.60
34	7.59	8.32	3.85	71	3.08	3.37	1.58
35	7.35	8.06	3.73	72	3.05	3.33	1.56
36	7.13	7.82	3.62				

**Table 3.** Results of peak and volume of each breach during a design flood with a 100-year return period

<b>River name</b>	<b>Name of breach</b>	<b>Discharge (m<sup>3</sup>/s)</b>	<b>Breach flood volume (10<sup>4</sup> m<sup>3</sup>)</b>
<b>Hougang River</b>	Hougang River left breach	148.38	590
	Hougang River main breach	161.86	645
<b>Xiatun River</b>	Xiatun River breach	78.49	298

According to the simulation analysis results, the overall height of the northern area of the airport is relatively high. The degree of submergence is relatively light. After the flood breaks, it will quickly evolve towards the low-lying areas in the central and southern parts, causing water accumulation and waterlogging. There are three main areas of severe waterlogging in the airport area. The first one is in the middle of the airport with a maximum submergence depth of 1.15m. The second location is located in the central eastern area of the airport, with a water depth of about 0.9m between vertex number 8 and 9. The third location is in the southwest area of the airport, with a maximum submergence depth of 1.32m. The degree of submergence in other areas within the simulated zone is considered as not significant.

The left branch of the Hougang River passes through the airport runway area, and the existing natural river channel cannot release the 100-year flood normally. When encountering the once-in-a-century flood, the flood will overflow and cause partial flooding of the airport area (near the strip submerged area numbered 10). Considering the safety of airport operations, it is recommended to widen the flood discharge section of the river during airport construction to ensure the smooth release of design floods and ensure the safety of airport flood discharge.

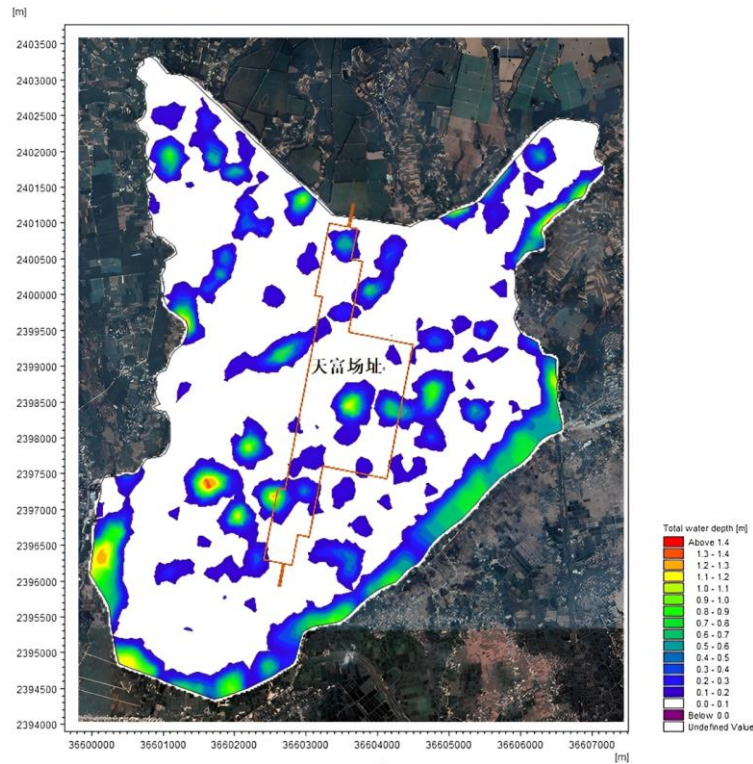


**Figure 6.** Results of maximum submerged depth in two-dimensional model

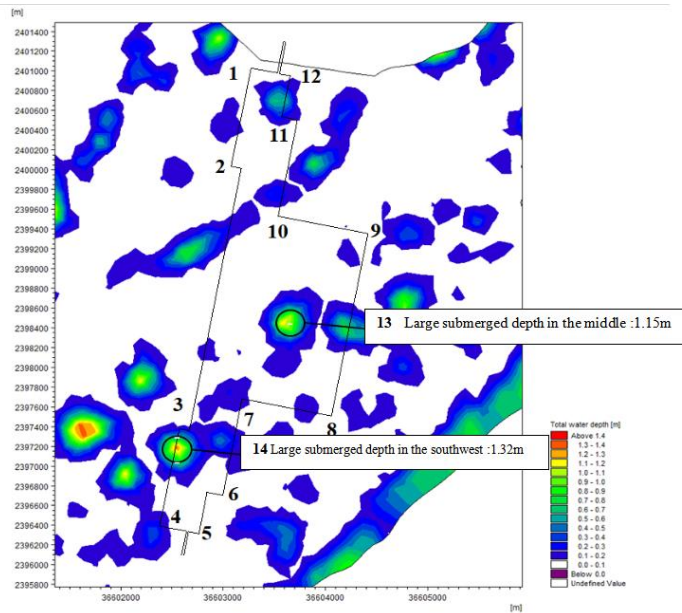


**Figure 7.** Schematic diagram of typical submerged locations within the proposed airport site

**Table 4.** Typical inundation results around the proposed airport (Unit: m)

Position	x	y	Natural ground level	Highest water level elevation	Maximum submergence depth
1	36603267.955	2400960.341	23.06		
2	36603185.775	2400031.078	21.20		
3	36602711.662	2397489.829	20.19	20.34	0.15
4	36602427.194	2396535.280	17.83	17.93	0.10
5	36602825.449	2396453.100	20.72		
6	36602939.236	2396927.214	19.66		
7	36603198.419	2397843.883	21.56	21.68	0.11
8	36603944.357	2397704.760	22.80		
9	36604292.041	2399474.785	23.28		
10	36603482.887	2399601.215	12.31		
11	36603653.568	2400524.156	19.91	20.06	0.15
12	36603723.104	2400909.769	22.15	22.25	0.10
13	36603590.353	2398457.021	22.13	23.27	1.15
14	36602547.302	2397186.396	17.88	19.20	1.32

**Note:** Areas with a submergence depth less than 0.1m are considered non-submerged areas, while areas with a depth greater than 0.1m are considered submerged areas.

#### 4. Conclusion

For this study, MIKE11 was used to construct one-dimensional models of the left branch of the Hougang River, the main stream of the Hougang River, and the Xiatusun River. MIKE21 was used to construct a two-dimensional flood routing model for the region. Considering the most unfavourable situation, the most unfavourable combination of three breach flood processes superimposed with regional rainstorm was used to analyse the flood risk that the proposed airport may encounter, and the following conclusions are obtained through simulation calculation:

(1) Under the comprehensive risk factors of the 100-year flood, the submerged water depth range within the site is 0-1.32m, where the submerged areas are mainly concentrated in the Southwest and central parts of the study area. There are three areas located on the southwest, central, and central eastern sides of the study area that resulted with significant submergence

depths. The maximum submergence depths are 1.32m, 1.15m, and 0.9m, respectively, but the range of maximum submergence depths is relatively small.

(2) When the left branch of the Hougang River crosses the airport runway and encounters a 100-year flood, a floodplain may appear. In order to ensure the safety of airport operation, it is recommended to appropriately expand the flood discharge section of the river during airport construction to ensure that floods do not affect the airport area.

(3) During the construction of the airport, it is necessary to appropriately cut and fill the site. It is recommended that the ground elevation after cutting and filling should not be lower than the flood and waterlogging height under the 100-year working condition. At the same time, proper drainage should be done within the site to avoid waterlogging.

### **Acknowledgement**

Not applicable

### **Credit Author Statement**

Conceptualization, C.T.; methodology, C.T.; software, C.T.; validation, C.T.; formal analysis, C.T.; investigation, C.T.; resources, C.T.; data curation, C.T.; writing—original draft preparation, C.T.; writing—review and editing, S.K.

### **Conflicts of Interest**

The authors declare no conflict of interest.

### **References**

- Chen, P., & Zhao, J. (2022). Analysis of the origins and countermeasures for urban waterlogging caused by rainstorms. *Journal of Catastrophology*. 37(3). 33–60.
- Ghaeini-Hessaroeeyeh, M., Namin, M.M., & Fadaei-Kermani, E. (2022). 2-D dam-break flow modeling based on weighted average flux method. *Iranian Journal of Science and Technology, Transactions of Civil Engineering*. 46(2). 1515–1525. <https://doi.org/10.1007/s40996-021-00708-6>
- Hasibuan, M.S., Widiatmaka, Tarigan, S.D., & Ambarwulan, W. (2022). Flood inundation distribution modelling for river boundary management in Cisadane sub-watershed. *IOP Conference Series: Earth and Environmental Science*. 1109(1). <https://iopscience.iop.org/article/10.1088/1755-1315/1109/1/012087>

- Hosseinzadehtalaei, P., Ishadi, N.K., Tabari, H., & Willems, P. (2021). Climate change impact assessment on pluvial flooding using a distribution-based bias correction of regional climate model simulations. *Journal of Hydrology*. 598. 126239. <https://doi.org/10.1016/j.jhydrol.2021.126239>
- Li, W. (2006). *Hydraulic calculation manual*. China: China Water Power Press.
- Li, Y. (2021). *Study on the characteristics of flood evolution due to dam breach of earth-rock dams in mountainous rivers* (Master's thesis). Chongqing: Chongqing Jiaotong University.
- Min, L., Shan, X., & Jiaxin, J. (2022). Risk analysis and response to urban waterlogging caused by extreme rainstorms in Wuhan. *China Flood & Drought Management*. 32(9). 46–50.
- Seyedashraf, O., Mehrabi, M., & Akhtari, A.A. (2018). Novel approach for dam break flow modeling using computational intelligence. *Journal of Hydrology*. 559. 1028–1038. <https://doi.org/10.1016/j.jhydrol.2018.03.001>
- Wang, W., Qin, W., & Lin, H.L. (2015). A review and outlook on urban waterlogging research in China. *Urban Issues*. 10. 24–28.
- Wanlin, H., & Zhen, W. (2022). Flood risk analysis in estuarine areas based on the Mike21 model. *Technical Supervision in Water Resources*. 7. 138–141.
- Wei, H., Liyuan, Z., & Liu, J. (2022). Hydrodynamic modelling and flood risk analysis of urban catchments under multiple scenarios: A case study of Dongfeng canal district, Zhengzhou. *International Journal of Environmental Research and Public Health*. 22(19). 14630. <https://doi.org/10.3390/ijerph192214630>
- Xueyao, L., & Cheng, G. (2019). Risk analysis of levee-break floods in small polder areas under different breach locations and forms. *Water Resources and Power*. 37(7). 46–121.
- Yang, K., Hou, H., Li, Y., Chen, Y., Wang, L., Wang, P., & Tangao, H. (2022). Future urban waterlogging simulation based on LULC forecast model: A case study in Haining City, China. *Sustainable Cities and Society*. 81. 104167. <https://doi.org/10.1016/j.scs.2022.104167>